Nov. 26-28, 2012 in Daejeon Convention Center(DCC), Daejeon, Korea

Controlling and Maximizing Humanoid Robot Pushing Force through Posture

Youngbum Jun[1], Alex Alspach[2] and Paul Oh[3]

[1,2,3]Mechanical Engineering and Mechanics, Drexel University, Philadelphia, PA 19104, USA
(E-mail: youngbum.jun@drexel.edu, alex.alspach@drexel.edu, paul@coe.drexel.edu)

Abstract - Pushing is one of many object manipulation strategies that requires interaction with the environment. Many force control approaches have been proposed for such manipulation. In a force controller implementation for a humanoid robot, however, there is no fixed base. If the required reaction force is greater than the humanoid robot can support, the robot will lose its balance. This paper presents a method to expand these force limits by changing a humanoid robot's posture. Based on Double Inverted Pendulum (DIP) model, the force limitation that the humanoid robot can support is calculated. With a feet-apart strategy and whole-body posture, a method is proposed to maximize the force limitation under the condition that the height of the target object is constant. Finally, comparison of simulation and experimental data validates the approach.

Keywords - Hubo, Whole-body Posture, Pushing, Force limitation

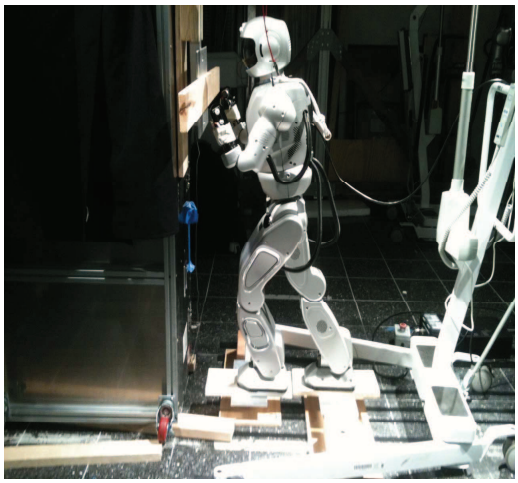

Fig. 1 Hubo+ (KHR) pushing a wall with the maximum posture in place

1. Introduction

The ability to apply a pushing force to an environment is a fundamental skill for a humanoid robot. While pushing force is generally used to move an object in a horizontal direction, it is also useful to manipulate a lot of mechanisms such as doors, wheelchairs, and dollies. It must be applied when using tools like drills or saws to guarantee proper action of the tool. Pushing is an act of a physical interaction that fundamentally follows Newton's third law. Many researchers in biomechanics [1] have investigated the factors that influence the magnitude of pushing force by measuring reaction forces on the environment. They concluded that the pushing force magnitude is mainly determined by the body's posture, and its maximum force is limited by the ability to displace the Center of Mass (CoM) from Center of Pressure (CoP) located on the support foot [1]. Based on such ideas, Harada et. al combined it with Zero-Moment Point (ZMP) stability criterion for the humanoid pushing [2].

The main interest in [2] was the humanoid pushing in walking. To achieve such goal, a full-sized humanoid robot was modeled as a Linearized Inverted Pendulum (LIPM), a common technique for modeling the dynamics of a bipedal robot. To control the pushing force, they moved the position of CoM forward and backward based on the force data on wrist. Impedance control on the arms prevented a humanoid robot from losing balance by producing a reaction force greater than the desired pushing force. This methodology has been extended over the past decade and resulted in a full-sized humanoid robot pushing a person in a wheelchair [3].

The previous works related to a pushing task have mainly focused on pushing in walking. This work extends existing algorithms to dynamic pushing in place. Pushing in place is useful for applications such as using hand and power tools, turning knobs and wheels, and manipulating controls. In these cases, a humanoid robot must delicately control the pushing force so as not to break an object or tool, or damage the robot. Many force control methods have been demonstrated [4] [5] to limit excessive forces due to position errors. The forces produced from these methods do not consider the additional limitation that a humanoid robot must balance over its support polygon. Without this consideration, large forces generated by the actuators or from the environment may push the robot over, despite being consistent with the force control model. Thus, it is important to understand the force limitation that the humanoid robot can support and how to maximize and control it.

This paper analyzes the relationship between pushing force and body postures, proposing a method to maximize possible pushing force for a given object height. Using a feet-apart strategy [1] and upper body placement, the force-posture relationship is derived for the case of static feet. Based on this relationship, the concept of maximum pushing posture is introduced. Through experiments with Drexel University's full-sized humanoid robot, Jaemi Hubo [6], author's approach is evaluated and the author validates that the force limitation significantly depends on the body postures and maximum pushing force can be achieved by utilizing the upper body.

2. Dynamic Model with External Force

Harada et. al [2] derived the linear relationship between the Zero-Moment Point (ZMP) and reaction force based on cart-table inverted pendulum model [8]. To better model the effects of the center of mass location compared to the foot and hand contacts of the robot, the ZMP model was expanded to work with the DIP model. This model considers the additional effects of the upper body location on the support polygon.

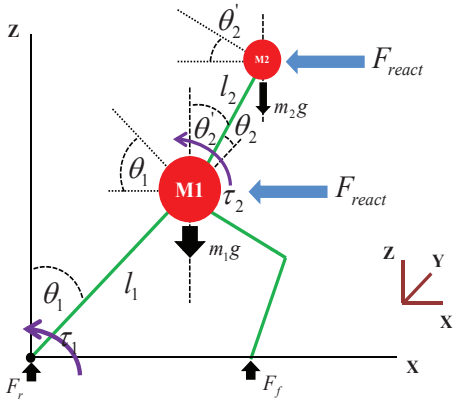

Fig. 2 A force model of Double Inverted Pendulum in a static posture

2.1 Double Inverted Pendulum Model

The Double Inverted Pendulum (DIP) [7] is one of several dynamic models to utilize the upper body. Figure. 2 represents a 2-dimensional kinematics and dynamics of DIP with the feet-apart posture. The origin in Figure. 2 stands for the ankle joint in the rear leg. m_1 and m_2 are lower body point mass and upper body point mass, respectively. In this paper, the author assumes that m_1 and m_2 are located in the hip and chest, respectively, and the lower body link, l_1, and upper body link, l_2, are rotating with respect to the ankle and hip joints, respectively, in the humanoid robot. τ_1 and τ_2 denote the torque acting on the ankle joint of the rear leg and the hip joint. The dynamic equation of DIP without the external force is (1).

$$\begin{bmatrix}\tau_1\\ \tau_2\end{bmatrix} = M(\theta)\ddot{\theta} + V(\theta,\dot{\theta}) + G(\theta) \tag{1}$$

Where M is 2×2 inertial matrix, V is 2×2 centrifugal and Coriolis part, and G is 2×2 gravitational constant.

Note that the torque acting on the ankle joint of the front foot is ignored since the location of the front foot will be determined by (7). It means that the contribution of that torque to the ZMP is very small when the external force is applied. Also note that the mass of the front leg is ignored in this model, but will affect the actual ZMP of the robot.

2.2 Relationship between Zero-Moment Point and External Force

In the static posture, the acceleration and velocity of the upper limbs and lower limb can be ignored. Accordingly, (1) remains only gravitational part and is shown as (2).

$$\begin{bmatrix}\tau_1\\ \tau_2\end{bmatrix} = \begin{bmatrix}-(m_1+m_2)l_1 g\sin(\theta_1) - m_2 l_2 g\sin(\theta_1+\theta_2)\\ -m_2 l_2 g\sin(\theta_1+\theta_2)\end{bmatrix} \tag{2}$$

In this case, the ZMP equation is simply defined as (3). Thus, the ZMP in the forward direction, X, is as shown as (4).

$$\frac{-\tau_1}{F_z} = ZMP = \frac{-\tau_1}{(m_1+m_2)g} \tag{3}$$

Where F_z is the ground reaction force that equals to $(m_1+m_2)g$.

$$ZMP_x = l_1\sin(\theta_1) + \frac{m_2}{m_1+m_2} l_2\sin(\theta_1+\theta_2) \tag{4}$$

With the external force, τ_1 which is the joint torque on the ankle of the rear leg is defined as in (2).

$$\tau_1 = -(m_1+m_2)l_1 g\sin(\theta_1) - m_2 l_2 g\sin(\theta_1+\theta_2) + \tau_{react}$$
$$\text{Where } \tau_{react} = F_{react}(l_1\cos(\theta_1) + l_2\cos(\theta_1+\theta_2)) \tag{5}$$

With (3), the important relationship between the horizontal reaction force in a given posture is derived in (6).

$$\frac{1}{a}\triangle ZMP = \triangle F_{react} \tag{6}$$
$$\text{Where } a = \frac{l_1\cos(\theta_1) + l_2\cos(\theta_1+\theta_2)}{(m_1+m_2)g}$$

Since $\theta_1+\theta_2$ are numeric values that can be obtained from a given posture. Thus, the relationship between the reaction force and ZMP is linear. It is the same result as in [2].

3. Feet-apart Strategy and Maximum Pushing Posture

The feet-apart strategy [1] is a posture with a stretched rear leg. Humans naturally use this strategy in many pushing tasks in order to maximize the pushing force. The effect of this posture is to extend the support polygon front-to-back, which allows the ZMP to be pushed farther back as well. Also, human changes the lower and upper body posture simultaneously to handle the magnitude of the maximum pushing force.

3.1 Feet-apart Posture on Humanoid Robot

The foot location of the rear leg can be easily calculated from the location of m_1. Now, the foot location of the front leg has to be determined. The front leg does not significantly affect the magnitude of the pushing force, but plays an important role in stability and manipulability of a humanoid robot while pushing. (7) is the boundary condition of minimum displacement of the front foot.

$$d \geqq \frac{(m_1+m_2)l_1 g\sin(\theta_1)+m_2 l_2 g\sin(\theta_1+\theta_2)}{(m_1+m_2)g} \tag{7}$$

Where d is the displacement from the rear foot location.

It is obvious that if the initial ZMP without the reaction force is further than the front foot, the humanoid robot will fall forward. Conversely, if the front leg is stretched toward the forward direction, the support polygon becomes largest. Due to the extreme stretch of the legs, however, the manipulability is the smallest at this pose, implying that the lower body cannot move and maintain the desired foot positions. Thus the front foot location should be determined based on the specific pushing task.

Note that it is important to align the rear foot and ZMP locations with the line of the force direction. If not, the humanoid robot will lose its balance.

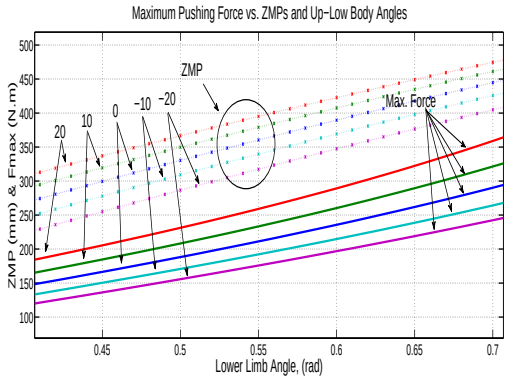

Fig. 3 Maximum pushing force vs. ZMP and Postures

3.2 Force Limitation

Based on (6), the ZMP is moving from the initially placed position to the rear support foot when pushing force is applying to the target object. Assume that friction is enough for the humanoid robot to tip over, the humanoid robot starts to tip while the ZMP is passing through the location of the rear foot. Mathematically such condition can be defined as $\tau_1 = 0$. Thus the pushing force of a given posture can be calculated using (3) and (8).

$$F_{max} = \frac{(m_1+m_2)l_1 g\sin(\theta_1)+m_2 l_2 g\sin(\theta_1+\theta_2)}{l_1\cos(\theta_1)+l_2\cos(\theta_1+\theta_2)} \tag{8}$$

Where F_{max} is the force limitation that the humanoid robot can support. As long as there is no vertical force pressing the humanoid robot down, (8) is valid. Thus, the force controller to manipulate the target object should be designed within the force limitations, and its performance should not exceed that force so as to maintain balance while carrying out a pushing task.

3.3 Posture for Maximum Pushing Force

In previous works [1][2][3], they controls the pushing force by horizontally changing the position of CoM while the upper body is upright to the ground in order to keep the height of the contact point between the arms and object. With this idea, the author controls the pushing force using both lower and upper body simultaneously while maintaining the height of the contact point.

Assume that the humanoid robot is at its initial pose, and the height of the target object is specified as in (9).

$$P_h = l_1\sin(\theta_1)+l_2\sin(\theta_1+\theta_2) = const. \tag{9}$$

Where P_h is the pushing height. All possible postures with the constant height will satisfy the condition shown in (10).

$$P_h = l_1\sin(\theta_1')+l_2\sin(\theta_1'+\theta_2') \tag{10}$$

Where θ_1' and θ_2' are the angle of the lower body and upper body, respectively. Using (10), the posture that has maximum pushing force in a given initial posture and height of the object can be obtained by (3).

$$max[\theta_1,\theta_2] = max\left(\frac{(m_1+m_2)l_1 g\sin(\theta_1')+m_2 l_2 g\sin(\theta_1'+\theta_2')}{l_1\cos(\theta_1')+l_2\cos(\theta_1'+\theta_2')}\right) \tag{11}$$

4. Simulation and Experiment

The Hubo+ humanoid robot developed by KAIST in South Korea is used for simulation and experiments. The maximum length from hip and ankle joint is 560mm, and the length of hip joint to chest is 367mm. The distance between center of the robot to hip joint in lateral direction is 88.5mm. The total weight is 47kg. Based on such parameters, the author set the lower body mass and upper body mass as 30kg and 17kg, respectively.

4.1 Simulation

Figure. 3 represents the simulation data of (8). The five dotted lines represent ZMP trajectories, while the five bold lines show push force limits (Max. Force) that correspond to the ZMP. The line at the top in the dotted group is the ZMP plot based on the lower body angle that varies from 0.45 to 0.7 rad and upper body angle that equals 20deg. The force plot corresponding to that ZMP plot is shown at the top in the bold group. In the same manner, each dotted line for ZMP from the bottom to the top shows the upper limb angle from -20, -10, 0, 10, and 20deg and corresponds to each bold line for force limitation from the bottom to the top, respectively.

There are two facts that must be emphasized. First, the force limitation of each posture is unique. Secondly, even if some postures have the same ZMP values, the force limitations are different from each other because of the different upper body angles. It gives an idea that there is an unique posture that can produce the maximum pushing force in accordance with the height of the contact point.

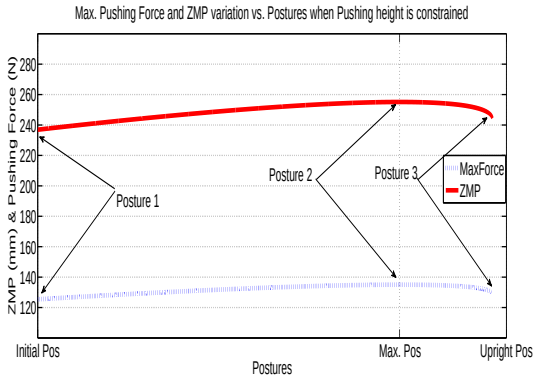

Fig. 4 Maximum pushing force and ZMP variation from posture 1 to posture 3

In Figure. 4 shows the pushing force and ZMP variation with the different posture when the contact point is specified. To clarify, the arrow named Posture 1 in Figure. 4 indicates the maximum pushing force (red and bold line) and ZMP (blue and dot line) of the robot posing (a) in Figure. 5. The arrow named Posture 2, and Posture 3 also point both maximum pushing force and ZMP, and corresponds to (b) and (c) in Figure. 5, respectively. (a) in Figure. 5 is the initial posture. (b) and (c) are the posture of the maximum pushing force and the upright posture obtained from (3),[3] respectively. Posture 1, (a) in Figure. 5, is the initial posture when $\theta_1 = 20\,\text{deg}$ and $\theta_2 = 0\,\text{deg}$. Posture 2, (b), shows the maximum pushing force posture when $\theta_1 = 24.63\,\text{deg}$ and $\theta_2 = -15.21\,\text{deg}$ and (c) is the upper body upright posture when $\theta_1 = 25.81\,\text{deg}$ and $\theta_2 = -25.60\,\text{deg}$.

In the simulation result in Figure. 4, there is an unique posture that can generate the maximum pushing force without changing the height of the contact point. Beyond our simulation, the humanoid robot can achieve the maximum pushing posture using lower and upper body angles.

4.2 Hubo+ Experimental Result

Figure. 5 shows the experimental set up. The reaction force and ground reaction force on each foot are recorded while Hubo+ is pushing the wall. Figure. 6 represents the reaction force vs. ZMP plot of posture 1, 2, and 3. The experimental data in Figure. 6 fits expectations based on the results of Figure. 4.

Figure. 7 describes the comparison between the simulation data in Figure. 4 and the experimental data. (a), (b), and (c) in Figure. 7 denotes posture 1, 2, and 3, respectively. The blue and bold line in each plot stands for the simulation data using DIP model and the read and dot line in each graph means the experimental data from Hubo+.

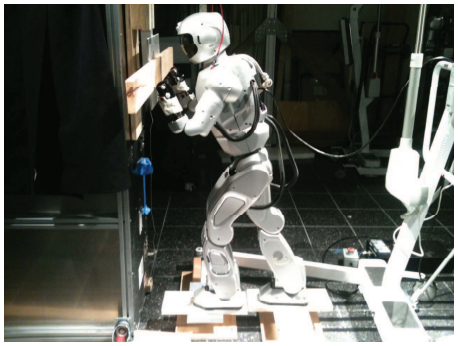

(a)

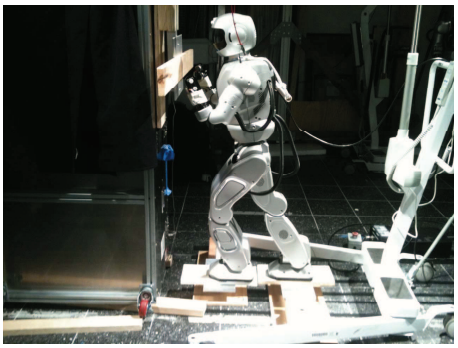

(b)

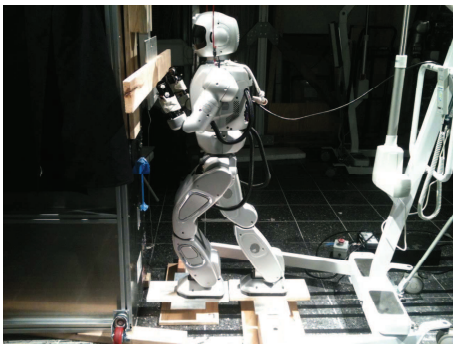

(c)

Fig. 5 Experiments. (a) Initial posture, (b) Maximum pushing posture, and (c) Upper body upright posture.

5. Conclusion

The author in this paper explained the force limitation in terms of the humanoid posture and proposed a method to maximize the pushing force. The idea was inspired by the human pushing motion. To maximize the pushing force, the author employed the feet-apart strategy to stretch the support leg in a static posture and controlled the lower and upper angles to obtain the posture that can produce the maximum pushing force. A Double Inverted Pendulum (DIP) model was used as a dynamic model of the humanoid robot. Based on such model, the relationship was demonstrated between the force limitation and Zero-Moment Point according to the posture. Through

the actual implementation on Hubo+, the proposed force analysis and postures were evaluated.

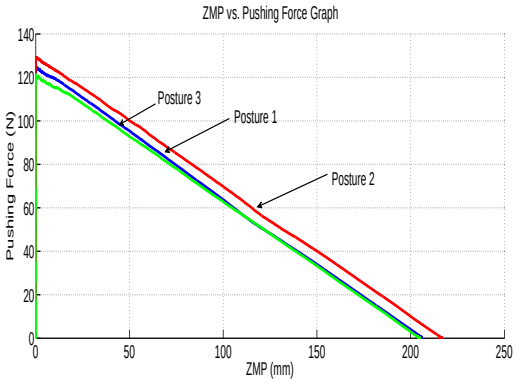

Fig. 6 ZMP vs. Pushing force

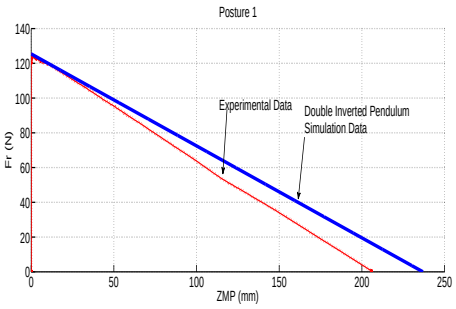

(a)

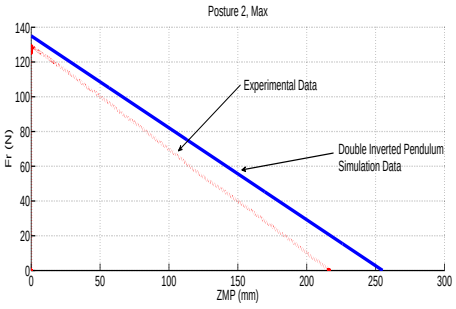

(b)

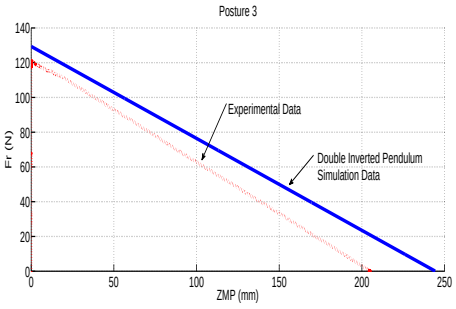

(c)

Fig. 7 ZMP vs. Pushing force. (a) Initial posture, (b) Maximum pushing posture, and (c) Upper body upright posture.

References

[1] Rancourt,Denis and Hogan,Neville, "Dynamics of Pushing", *Journal of motor behavior*, V33, N4, pp.351-362, 2001

[2] Harada, K.; Kaneko, M., "Whole body manipulation", *Intelligent Syst. Inst., Nat. Inst. of Adv. Ind. Sci. and Technol.*, V1, pp.190-195, 2003, Tsukuba, Japan

[3] Nozawa, S., Kakiuchi, Y., Okada, K., Inaba, M. "Controlling the planar motion of a heavy object by pushing with a humanoid robot using dual-arm force control", *Robotics and Automation, ICRA, IEEE Int. Conf. on*,pp.1428-1435, 2004, Saint Paul, MN, USA

[4] Hogan, N., "Impedance Control: An Approach to Manipulation: Part I - Theory", pp. 1-7, "Part II -Implementation", pp. 8-16, "Part 111 - Applications", pp. 17-24, *ASME Journal of Dynamic Systems, Measurement and Control*, Nov. 107, 1985

[5] Whitney, D. (1977) "Force Feedback Control of Manipulator Fine Motions", *Journal of Dynamic Systems, Measurement and Control*, pp. 91-97

[6] Kim, J.H., Oh, J.H.,"Walking Control of the Humanoid Platform KHR-1 based on Torque Feedback Control", *IEEE International Conference on Robotics and Automation (ICRA)*, Barcelona, Spain, April 2004.

[7] Napoleon, Shigeki, N., Mitsuji, S., "Balance Control Analysis of Humanoid Robot based on ZMP Feedback Control", *Int. Conf. on Intelligent Robots and Systems*, V3, pp.2437-2442, 2002, Lausanne, Switzerland

[8] Kajita, S., Kanehiro, F., Kaneko, K., Fujiwara, K., Harada, K., Yokoi, K., Hirukawa, H., "Biped Walking Pattern Generation Using Preview Control of the Zero-Moment-Point", *IEEE Int. Conf. on Robotics and Automation (ICRA2003)*, Taipei, Taiwan, V2, pp.1620-1626, Sept. 2003